



Nonreciprocal mechanical squeezing in a spinning cavity optomechanical system via pump modulation

Qi Guo ^{1,2,*} Ke-Xin Zhou,^{1,2} Cheng-Hua Bai,³ Yuchi Zhang,^{1,2} Gang Li ^{1,2} and Tiancai Zhang^{1,2,†}

¹*State Key Laboratory of Quantum Optics and Quantum Optics Devices, Institute of Opto-Electronics, College of Physics and Electronic Engineering, Shanxi University, Taiyuan, Shanxi 030006, China*

²*Collaborative Innovation Center of Extreme Optics, Shanxi University, Taiyuan 030006, China*

³*Department of Physics, School of Science, North University of China, Taiyuan, Shanxi 030051, China*



(Received 18 May 2023; revised 11 August 2023; accepted 8 September 2023; published 19 September 2023)

We propose a scheme to realize nonreciprocal mechanical squeezing in a spinning optomechanical system, where a spinning resonator is driven by a periodically modulated laser field via a tapered optical fiber. The spinning resonator supports two counterpropagating optical modes and a mechanical breathing mode induced by the radiation pressure. According to the optical Sagnac effect, the two counterpropagating optical modes obtain opposite frequency shifts. By utilizing the modulated pump field with a given frequency, mechanical squeezing can only be achieved by driving the resonator from one direction but not from the other. We analyze the impact of backscattering losses on mechanical squeezing and find that this negative impact can be almost completely avoided by increasing the angular velocity of the resonator. We also show that the presented scheme is robust to mechanical thermal noise and can be realized under the current experimental conditions. Therefore, this work may be meaningful for the study of quantum nonreciprocity and quantum precision measurement.

DOI: [10.1103/PhysRevA.108.033515](https://doi.org/10.1103/PhysRevA.108.033515)

I. INTRODUCTION

Nonreciprocal physics, which refers to the phenomenon that a system behaves differently in opposite directions, has attracted increasing research interest in recent years. The study of nonreciprocity has been extended to various branches of physics, such as acoustics [1,2], optics [3], thermodynamics [4], etc. In particular, optical nonreciprocity has attracted a lot of attention. Traditional optical nonreciprocal transmission schemes are mainly achieved by using the Faraday effect in magneto-optical crystal materials [5], which usually requires a strong magnetic field [2]. In recent years, a variety of optical nonreciprocity schemes based on nonmagnetic materials have been proposed in theory and experiments by employing optical nonlinearities, such as Kerr nonlinearity [6–8], radiation-pressure-coupled optomechanics [9–13], Brillouin scattering [14,15], stimulated Raman scattering [16], light-atom strong coupling [17], and so on.

Quantum nonreciprocal effects have also been an important topic because the realization of nonreciprocal quantum devices can provide new opportunities to study fundamental physics and promote the development of quantum information processing and quantum computing. Recently, quantum nonreciprocal engineering has made great progress at the single-photon level [18–25], which has laid the foundation for further study of the nonreciprocal control of quantum states and quantum fluctuations. On the other hand, the cavity optomechanics (COM) system provides an ideal platform for

the study of nonreciprocity [26–28]. In particular, the spinning COM system exhibits unique properties superior to other systems in studying both classical and quantum nonreciprocity. For example, the nonreciprocal propagation of light with 99.6% isolation was experimentally demonstrated by using such a spinning device [27]. The nonreciprocal quantum entanglement between light and motion [29] and between two distant mechanical oscillators [30] was proposed based on the spinning resonator, where counterintuitive robustness against random losses and nonreciprocal entanglement enhancement were revealed respectively. The nonreciprocal phonon laser was demonstrated in a spinning COM system [31] and a spinning microwave magnomechanical system [32]. In addition, many other nonreciprocal quantum properties in the spinning COM system, e.g., nonreciprocal photon blockade [33,34] and nonreciprocal mechanical squeezing [35], have also been studied theoretically.

The mechanical squeezing, one of the most important nonclassical properties in optomechanical systems, has been widely studied through different methods of introducing nonlinearities, such as parametrically driving [36,37], two-tone driving [38], pump modulation [39–47], Duffing nonlinearity [48,49], etc. Among these methods, pump modulation has been extended to produce more interesting quantum properties and quantum dynamics [50–52]. Motivated by these works, in this paper, we combine the spinning resonator and the periodic amplitude modulation of the driving field to present a scheme for realizing the nonreciprocal mechanical squeezing; i.e., the mechanical squeezing can be achieved by driving the resonator from one direction but not from the other. Moreover, we study the effects of backscattering losses and the environmental temperature on the mechanical squeezing. It is

*qguo@sxu.edu.cn

†tczhang@sxu.edu.cn

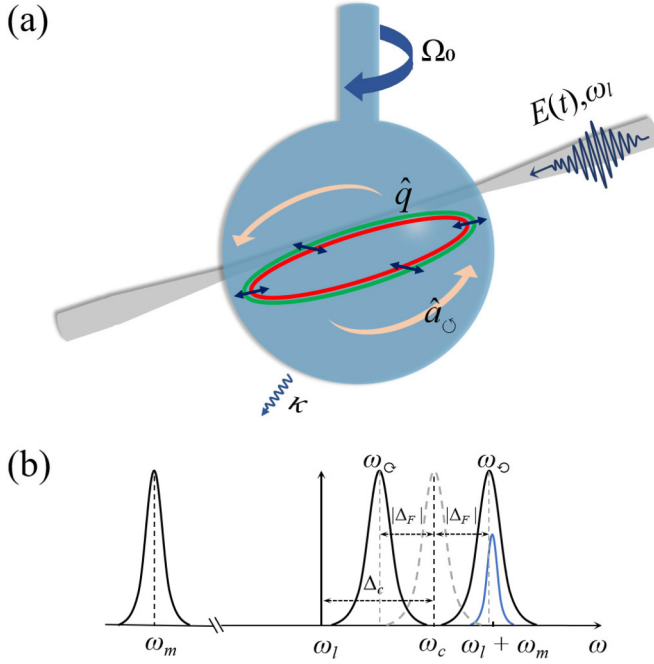


FIG. 1. (a) Schematic diagram for the spinning optomechanical system. The resonator is fixed to rotate clockwise, and the external laser with the frequency ω_l and the time-dependent amplitude $E(t)$ enters the tapered fiber from the left (right)-hand side to drive the CW (CCW) mode. The CW and CCW modes are coupled via backscattering with the strength J . (b) Frequency spectrum of the spinning optomechanical system, where $\Delta_c = \omega_c - \omega_l$.

found that the nonreciprocal mechanical squeezing has strong robustness against backscattering losses and thermal noise, and is almost unaffected by backscattering losses for large rotational angular velocities. Even if the environmental temperature reaches several hundred millikelvins, the squeezing is still present.

This paper is organized as follows. In Sec. II, we describe the proposed model of the spinning COM system in detail and obtain the linearized quantum Langevin equations. In Sec. III, we derive the evolution equation of the covariance matrix corresponding to the system quadratures and show how to generate nonreciprocal mechanical squeezing. In Sec. IV, we demonstrate the robustness of nonreciprocal mechanical squeezing against backscattering losses and thermal noise. Finally, conclusions are presented in Sec. V.

II. THEORETICAL MODEL AND THE DYNAMICS OF THE SPINNING OPTOMECHANICAL SYSTEM

We consider a COM system as shown schematically in Fig. 1, where a spinning resonator is transiently coupled with a tapered fiber. The periodically amplitude-modulated laser is fed into the fiber from the left-hand side or the right-hand side and drives the clockwise (CW) mode and the counterclockwise (CCW) mode of the resonator through an evanescent field, and the resonator supports a radiation-pressure-induced mechanical radial breathing mode with the frequency ω_m . Due to the optical Sagnac effect induced by the spinning, the two degenerate counterpropagating optical modes in the resonator

will be broken by opposite Sagnac-Fizeau shifts [27,53] with respect to the resonance frequencies ω_c for a stationary resonator, i.e., $\omega_c \rightarrow \omega_c + \Delta_F$, with

$$\Delta_F = \pm \Omega_0 \frac{nR\omega_c}{c} \left(1 - \frac{1}{n^2} - \frac{\lambda}{n} \frac{dn}{d\lambda} \right), \quad (1)$$

where $n(R)$ is the refractive index (radius) of the resonator, Ω_0 is the angular velocity of the resonator, and c (λ) is the speed (wavelength) of light in the vacuum. The dispersion term $dn/d\lambda$ characterizes the relativistic origin of the Sagnac effect and can usually be ignored because it is small in typical materials [27,53]. The Sagnac-Fizeau shift is proportional to the rotational speed and the radius of the cavity. The “+” and the “−” at the beginning of the right-hand side of Eq. (1) correspond to the shift of the optical mode propagating against and along the rotation direction of the resonator, respectively. When the driving laser is fed into the fiber from the CCW direction, the Hamiltonian of the spinning optomechanical system is

$$\begin{aligned} \hat{H} &= \hat{H}_0 + \hat{H}_{\text{int}} + \hat{H}_{\text{dr}}, \\ \hat{H}_0 &= \hbar \sum_{j=\cup, \cup} \omega_j \hat{a}_j^\dagger \hat{a}_j + \frac{\hbar \omega_m}{2} (\hat{p}^2 + \hat{q}^2), \\ \hat{H}_{\text{int}} &= \hbar J (\hat{a}_\cup^\dagger \hat{a}_\cup + \hat{a}_\cup^\dagger \hat{a}_\cup) - \hbar G_0 (\hat{a}_\cup^\dagger \hat{a}_\cup + \hat{a}_\cup^\dagger \hat{a}_\cup) \hat{q}, \\ \hat{H}_{\text{dr}} &= i\hbar [E(t) \hat{a}_\cup^\dagger e^{-i\omega_l t} - E^*(t) \hat{a}_\cup e^{i\omega_l t}]. \end{aligned} \quad (2)$$

Here, ω_m , $\omega_{\cup(\cup)} \equiv \omega_c \pm |\Delta_F|$, and ω_l are the frequencies of the mechanical mode, the CCW (CW) cavity mode for the CW spinning resonator, and the driving laser, respectively. \hat{a}_j (\hat{a}_j^\dagger) is the annihilation (creation) operator of the optical mode j ($j = \cup, \cup$), and \hat{q} (\hat{p}) is the dimensionless mechanical displacement (momentum) operator. $G_0 = (\omega_c/R) \times \sqrt{\hbar/m\omega_m}$ denotes the single-photon COM coupling rate, with m being the mass of the resonator [54]. The coupling between the CW mode and the CCW mode is described by the mode-coupling strength J caused by the Rayleigh backscattering due to the imperfections of devices [55,56]. The amplitude of the external laser $E(t)$ is periodically modulated with the period τ [$E(t) = E(t + \tau)$]; therefore, Fourier series expansion can be performed on the periodically modulated amplitude $E(t) = \sum_{n=-\infty}^{\infty} E_n e^{-in\Omega t}$, where $\Omega = 2\pi/\tau$ ($\tau > 0$) is the fundamental modulation frequency. The modulation coefficients $E_n = \sqrt{2\kappa P_n/\hbar\omega_l}$, where P_n and κ are the power of the associated sidebands and the decay rate of the optical mode, respectively. Without loss of generality, we truncate the series of the modulated amplitude $E(t)$ to $|n| \leq 1$, that is, adding a sinusoidal modulation to the input amplitude $E(t) = E_0 + 2E_1 \cos(\Omega t)$ (for $E_{-1} = E_1$), which can also be seen as a good approximation under the case that high sidebands fall outside the cavity bandwidth ($|n|\Omega > 2\kappa$ for $|n| \geq 2$).

In a rotating frame with respect to $\hat{H}_0 = \hbar\omega_l(\hat{a}_\cup^\dagger \hat{a}_\cup + \hat{a}_\cup^\dagger \hat{a}_\cup)$, the Hamiltonian of this spinning COM system ($\hbar = 1$) is

$$\begin{aligned} \hat{H} &= \sum_{j=\cup, \cup} \Delta_j \hat{a}_j^\dagger \hat{a}_j + \frac{\omega_m}{2} (\hat{p}^2 + \hat{q}^2) + J(\hat{a}_\cup^\dagger \hat{a}_\cup + \hat{a}_\cup^\dagger \hat{a}_\cup) \\ &\quad - G_0(\hat{a}_\cup^\dagger \hat{a}_\cup + \hat{a}_\cup^\dagger \hat{a}_\cup) \hat{q} + i[E(t) \hat{a}_\cup^\dagger - E^*(t) \hat{a}_\cup], \end{aligned} \quad (3)$$

where $\Delta_j = \omega_j - \omega_l$ is the detuning between the resonance frequency of the cavity field and the driving frequency. By taking the mechanical damping and cavity decay into account, the dissipative dynamics of the spinning COM system can be described by the following quantum Langevin equations (QLEs):

$$\begin{aligned}\dot{\hat{a}}_\cup &= -(i\Delta_\cup + \kappa)\hat{a}_\cup - iJ\hat{a}_\cup + iG_0\hat{a}_\cup\hat{q} + E(t) + \sqrt{2\kappa}\hat{a}_\cup^{\text{in}}, \\ \dot{\hat{a}}_\cup &= -(i\Delta_\cup + \kappa)\hat{a}_\cup - iJ\hat{a}_\cup + iG_0\hat{a}_\cup\hat{q} + \sqrt{2\kappa}\hat{a}_\cup^{\text{in}}, \\ \dot{\hat{q}} &= \omega_m\hat{p}, \\ \dot{\hat{p}} &= -\omega_m\hat{q} - \gamma_m\hat{p} + G_0(\hat{a}_\cup^\dagger\hat{a}_\cup + \hat{a}_\cup^\dagger\hat{a}_\cup) + \hat{\xi}(t),\end{aligned}\quad (4)$$

where γ_m is the mechanical damping rate, and \hat{a}_j^{in} and $\hat{\xi}(t)$ are the zero-mean input noise operator for the optical mode and the zero-mean Brownian motion noise operator, respectively, characterized by the following correlation functions [57–59]:

$$\begin{aligned}\langle \hat{a}_j^{\text{in}}(t)\hat{a}_j^{\text{in}\dagger}(t') \rangle &= \delta(t-t'), \quad \langle \hat{a}_j^{\text{in}\dagger}(t)\hat{a}_j^{\text{in}}(t') \rangle = 0, \\ \langle \hat{\xi}(t)\hat{\xi}(t') \rangle &= \frac{\gamma_m}{2\pi\omega_m} \\ &\times \int \left[\coth\left(\frac{\hbar\omega}{2k_B T}\right) + 1 \right] \omega e^{-i\omega(t-t')} d\omega,\end{aligned}\quad (5)$$

where k_B is the Boltzmann constant and T is the environmental temperature. For the mechanical oscillator with a high-quality factor $Q = \omega_m/\gamma_m \gg 1$, by Markovian approximation, the above correlation function of $\hat{\xi}(t)$ can be described as [59]

$$\langle \hat{\xi}(t)\hat{\xi}(t') + \hat{\xi}(t')\hat{\xi}(t) \rangle / 2 \simeq \gamma_m(2n_m + 1)\delta(t-t'), \quad (6)$$

where $n_m = [\exp(\hbar\omega_m/k_B T) - 1]^{-1}$ is the mean thermal phonon number. Under the condition of strong laser driving, we can linearize the dynamics by expanding each operator as a sum of its classical c -number first moment and a small fluctuation around it; i.e., $\hat{a}_j = \alpha_j + \delta\hat{a}_j$, $\hat{q} = q_s + \delta\hat{q}$, and $\hat{p} = p_s + \delta\hat{p}$. By substituting it into Eq. (4), we can obtain the evolution equations of the first moments:

$$\begin{aligned}\dot{\alpha}_\cup &= -(\kappa + i\tilde{\Delta}_\cup)\alpha_\cup - iJ\alpha_\cup + E(t), \\ \dot{\alpha}_\cup &= -(\kappa + i\tilde{\Delta}_\cup)\alpha_\cup - iJ\alpha_\cup, \\ \dot{q}_s &= \omega_m p_s, \\ \dot{p}_s &= -\omega_m q_s - \gamma_m p_s + G_0(|\alpha_\cup|^2 + |\alpha_\cup|^2),\end{aligned}\quad (7)$$

and the linearized QLEs of the quantum fluctuation operators are

$$\begin{aligned}\delta\dot{\hat{a}}_\cup &= -(\kappa + i\tilde{\Delta}_\cup)\delta\hat{a}_\cup - iJ\delta\hat{a}_\cup + iG_0\alpha_\cup\delta\hat{q} + \sqrt{2\kappa}\hat{a}_\cup^{\text{in}}, \\ \delta\dot{\hat{a}}_\cup &= -(\kappa + i\tilde{\Delta}_\cup)\delta\hat{a}_\cup - iJ\delta\hat{a}_\cup + iG_0\alpha_\cup\delta\hat{q} + \sqrt{2\kappa}\hat{a}_\cup^{\text{in}}, \\ \delta\dot{\hat{q}} &= \omega_m\delta\hat{p}, \\ \delta\dot{\hat{p}} &= -\omega_m\delta\hat{q} - \gamma_m\delta\hat{p} + G_0(\delta\hat{a}_\cup^\dagger\alpha_\cup + \alpha_\cup^*\delta\hat{a}_\cup \\ &+ \delta\hat{a}_\cup^\dagger\alpha_\cup + \alpha_\cup^*\delta\hat{a}_\cup) + \hat{\xi}(t),\end{aligned}\quad (8)$$

where $\tilde{\Delta}_j = \Delta_j - G_0q_s$ is the effective optical detuning.

III. GENERATION OF THE NONRECIPROCAL MECHANICAL SQUEEZING

Then, to solve the quantum fluctuation dynamics of the system more conveniently, we introduce the quadrature operators of the cavity modes and the corresponding input noise operators:

$$\begin{aligned}\delta\hat{X}_j &= \frac{1}{\sqrt{2}}(\delta\hat{a}_j^\dagger + \delta\hat{a}_j), \quad \delta\hat{Y}_j = \frac{i}{\sqrt{2}}(\delta\hat{a}_j^\dagger - \delta\hat{a}_j), \\ \hat{X}_j^{\text{in}} &= \frac{1}{\sqrt{2}}(\hat{a}_j^{\text{in}\dagger} + \hat{a}_j^{\text{in}}), \quad \hat{Y}_j^{\text{in}} = \frac{i}{\sqrt{2}}(\hat{a}_j^{\text{in}\dagger} - \hat{a}_j^{\text{in}}),\end{aligned}\quad (9)$$

and all the quadrature operators and corresponding noise operators can be expressed as the column vectors:

$$\begin{aligned}u^T(t) &= (\delta\hat{q}, \delta\hat{p}, \delta\hat{X}_\cup, \delta\hat{Y}_\cup, \delta\hat{X}_\cup, \delta\hat{Y}_\cup), \\ n^T(t) &= (0, \hat{\xi}(t), \sqrt{2\kappa}\hat{X}_\cup^{\text{in}}, \sqrt{2\kappa}\hat{Y}_\cup^{\text{in}}, \sqrt{2\kappa}\hat{X}_\cup^{\text{in}}, \sqrt{2\kappa}\hat{Y}_\cup^{\text{in}}).\end{aligned}\quad (10)$$

We rewrite the linearized QLEs of the quantum fluctuations in a compact form,

$$\dot{u}(t) = A(t)u(t) + n(t), \quad (11)$$

where $A(t)$ is a 6×6 time-dependent matrix

$$A(t) = \begin{bmatrix} 0 & \omega_m & 0 & 0 & 0 & 0 \\ -\omega_m & -\gamma_m & G_\cup^x(t) & G_\cup^y(t) & G_\cup^x(t) & G_\cup^y(t) \\ -G_\cup^y(t) & 0 & -\kappa & \tilde{\Delta}_\cup & 0 & J \\ G_\cup^x(t) & 0 & -\tilde{\Delta}_\cup & -\kappa & -J & 0 \\ -G_\cup^y(t) & 0 & 0 & J & -\kappa & \tilde{\Delta}_\cup \\ G_\cup^x(t) & 0 & -J & 0 & -\tilde{\Delta}_\cup & -\kappa \end{bmatrix}, \quad (12)$$

and $G_j^x(t)$ [$G_j^y(t)$] is the real [imaginary] part of the effective COM coupling rate $G_j(t) \equiv \sqrt{2}G_0\alpha_j = G_j^x(t) + iG_j^y(t)$.

Because of the linearized dynamics of the quantum fluctuations and the zero-mean Gaussian nature of the quantum noises, the asymptotic quantum state of the system will evolve into a Gaussian state independent of the initial states [60] and can be completely described by the 6×6 covariance matrix (CM) $v(t)$, whose elements are defined as

$$v_{kl} = \langle u_k(t)u_l(t) + u_l(t)u_k(t) \rangle / 2. \quad (13)$$

We can derive the motion equation of the CM $v(t)$ according to Eqs. (11) and (13):

$$\frac{dv}{dt} = A(t)v(t) + v(t)A(t)^T + D, \quad (14)$$

where $A(t)^T$ denotes the transpose of $A(t)$, and D is a diffusion matrix whose elements are related to noise correlation functions and defined as

$$\delta(t-t')D_{kl} = \langle n_k(t)n_l(t') + n_l(t')n_k(t) \rangle / 2. \quad (15)$$

From Eqs. (5) and (6), we find that D is a diagonal matrix:

$$D = \text{diag}[0, \gamma_m(2n_m + 1), \kappa, \kappa, \kappa, \kappa]. \quad (16)$$

Now the quantum properties of the system can be completely revealed by solving the CM $v(t)$. In the following

calculations, all eigenvalues of $A(t)$ have a negative real part for all time to ensure the stability of the system according to the Routh-Hurwitz criterion [61].

We now investigate the mechanical squeezing in the spinning optomechanical system with a periodically modulated pump. Due to the zero mean of the quantum fluctuations, the first and second diagonal elements of the CM $v(t)$ represent the variance of position and momentum operators of the mechanical oscillator, respectively. According to the Heisenberg uncertainty principle and the commutative relation $[\hat{q}, \hat{p}] = i$, as long as the variance $\langle \delta q^2 \rangle$ or $\langle \delta p^2 \rangle$, i.e., the first or second diagonal elements of the CM $v(t)$, is less than 0.5, it can be certified that mechanical squeezing is generated.

To achieve nonreciprocal mechanical squeezing in the CW spinning resonator, i.e., the mechanical squeezing can be generated by driving the CCW optical mode but not the CW optical mode, we should choose the driving frequency that satisfies $\tilde{\Delta}_\cup = \omega_m$, corresponding to the well-known sideband cooling setting. By straightforward calculations, this driving condition can also be written as $\Delta_c = \omega_m + G_0 q_s - |\Delta_F| \simeq 1.2\omega_m - |\Delta_F|$. Here the backscattering is not considered, i.e., assuming $J = 0$. We numerically calculate the position variance $\langle \delta q^2 \rangle$ of the mechanical mode and plot the evolution of the steady-state variance from $t = 596\tau$ to $t = 600\tau$ in Fig. 2(a), where we choose experimentally feasible parameters while ensuring system stability [27,62–64]: $n = 1.48$, $m = 10$ ng, $R = 1.1$ mm, $\lambda = 1.55$ μm , $Q = \omega_c/\kappa = 3.2 \times 10^7$, $\omega_m = 80$ MHz, $\gamma_m = 520$ Hz, $T = 0.05$ K, $\Omega_0 = 8$ kHz, $P_0 = 10$ mW, $P_{\pm 1} = 2$ mW, and the modulation frequency $\Omega = 2\omega_m$. The choice of the optimal modulation frequency and the effects of driving powers on the mechanical squeezing are analyzed in detail in the Appendix. The red (dashed) and blue (solid) lines represent the variances corresponding to the cases in which the cavity is driven from the left-hand side and the right-hand side, respectively. Obviously, when the driving direction is CCW, the position quadrature of the mechanical oscillator is periodically squeezed with the same period as the amplitude modulation. However, when the driving direction is CW, the mechanical squeezing is not generated. That is, the nonreciprocal mechanical squeezing can be achieved in this spinning optomechanical system.

The underlying physics can be understood as follows. According to the optical Sagnac effect, the spinning of the resonator will lead to the opposite Sagnac-Fizeau shifts for the two degenerate counterpropagating optical modes in the resonator, as shown in Fig. 1(b). For the resonator CW, if the CCW optical mode is driven by a red-detuned laser with the effective detuning $\tilde{\Delta}_\cup = \omega_m$, the anti-Stokes sideband scattered by the mechanical mode will be in resonance with the CCW optical mode and thus the mechanical mode can be cooled. However, if the same laser is used to drive the CW optical mode, the anti-Stokes sideband is detuned with the CW optical mode by $2|\Delta_F|$ as shown in Fig. 1(b), so the mechanical mode cannot be cooled. This nonreciprocal cooling is the foundation of the nonreciprocal mechanical squeezing. When the amplitude of the driving laser is modulated periodically with the frequency $\Omega = 2\omega_m$, according to Floquet's theorem, the spring constant of the mechanical motion will vary in time with the same frequency Ω (i.e., just twice the frequency of the mechanical mode), reminiscent of parametric amplification,

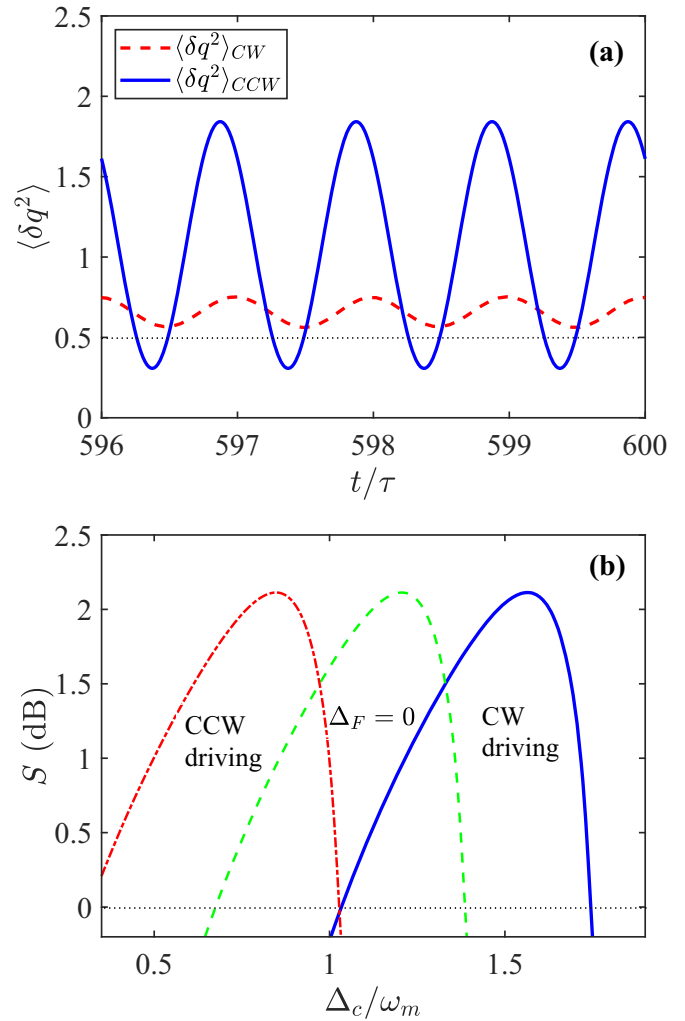


FIG. 2. (a) The evolution of the position variance of the mechanical mode with time without backscattering, where the angular velocity of the resonator is $\Omega_0 = 8$ kHz. The red (dashed) and blue (solid) lines correspond to the cases where the cavity is driven from the left-hand side and the right-hand side, respectively. The black dash-dotted line represents the standard quantum limit. (b) S (dB) versus Δ_c/ω_m for the spinning resonator ($\Omega_0 = 8$ kHz) with different driving directions (the red dot-dashed line and the blue solid line) and the stationary resonator (the green dashed line). These curves for S are asymmetric, because the redshift of the cavity mode induced by the optomechanical coupling is related to frequencies of the system. See the text for other parameters.

which will lead to the squeezing of the mechanical mode [39]. Therefore, by combining the spinning resonator and the pump modulation, the nonreciprocal mechanical squeezing can be achieved.

For a clearer presentation of the nonreciprocal mechanical squeezing, we express the maximal squeezing degree of the position quadrature in dB units, i.e., $S = -10 \log_{10} \frac{\langle \delta q^2 \rangle_{\min}}{\langle \delta q^2 \rangle_{\text{vac}}}$, with $\langle \delta q^2 \rangle_{\text{vac}} = \frac{1}{2}$ being the position variance of the mechanical mode in the ground state and $\langle \delta q^2 \rangle_{\min}$ being the minimum position variance. We plot the degree of squeezing S as a function of the detuning Δ_c for different driving directions in Fig. 2(b), in which the system parameters are the same

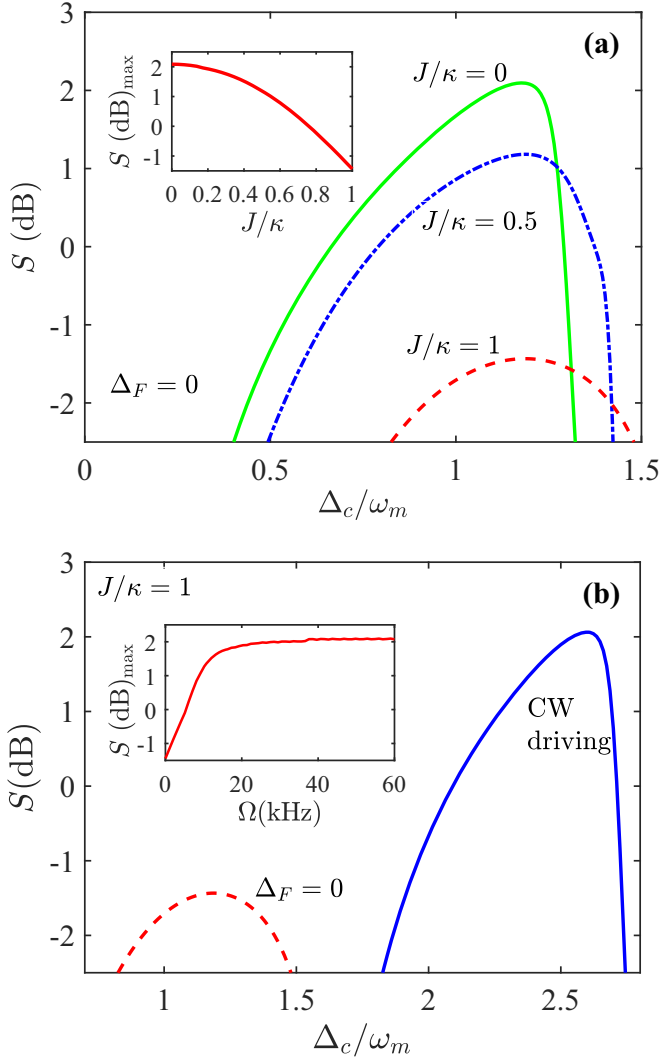


FIG. 3. (a) The influence of backscattering losses on the mechanical squeezing for the stationary resonator. (b) The nonreciprocal revival of the mechanical squeezing by spinning the resonator. The red dashed line and the blue solid line correspond to the squeezing for the stationary resonator and the CW spinning resonator with $\Omega_0 = 30$ kHz, respectively, for $J/\kappa = 1$. The other parameters are the same as those in Fig. 2.

as those in Fig. 2(a) except for Δ_c . The green (dashed) line represents the degree of squeezing for the stationary resonator, which is independent of the driving direction. The red (dot-dashed) line and the blue (solid) line correspond to the cases for the CW spinning resonator driven from the CCW and CW directions, respectively, which shows the nonreciprocity of the mechanical squeezing. For example, for Δ_c in the left region of Fig. 2(b), mechanical squeezing can be generated by driving the resonator from the CCW direction but not from the CW direction; for Δ_c in the right region, the opposite is true.

IV. NONRECIPROCAL MECHANICAL SQUEEZING AGAINST BACKSCATTERING LOSSES AND THERMAL NOISE

The nonreciprocal mechanical squeezing above is generated in an ideal COM system. However, for actual COM

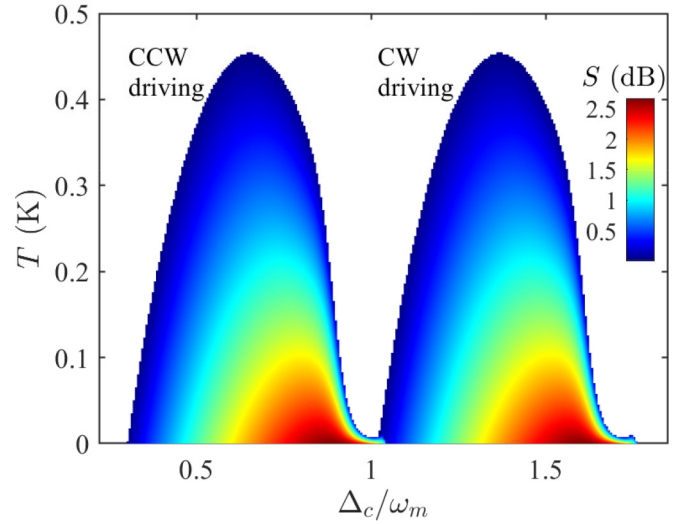


FIG. 4. The degree of squeezing S (dB) for the CW spinning resonator driven from the CCW and CW directions versus the environmental temperature T and the scaled detuning Δ_c/ω_m , where $\Omega_0 = 8$ kHz and $J/\kappa = 0$. The other parameters are the same as those in Fig. 2.

devices, imperfect factors inevitably exists, such as surface roughness or material defects, which will cause backscattering of the propagating light, leading to coupling between the counterpropagating optical modes, i.e., $J \neq 0$. In this section, we first discuss the effect of backscattering on the mechanical squeezing and study how to avoid such an effect. Figure 3(a) exhibits the mechanical squeezing for the stationary resonator with different backscattering strengths $J/\kappa = 0, 0.5$, and 1 , which shows that the degree of squeezing decreases sharply with increasing J . When J reaches approximately 0.8 , the squeezing will be absent, as shown in the inset of Fig. 3(a). Fortunately, we find that the influence of backscattering can be resisted effectively by spinning the resonator, as shown in Fig. 3(b), where the backscattering strength $J/\kappa = 1$. The red dashed line represents the squeezing for the stationary resonator [the same as the red dashed line in Fig. 3(a)], and the blue solid line is the squeezing for the CW spinning resonator with the angular velocity $\Omega_0 = 30$ kHz and CW driving. When we use the same pump to drive the CCW mode of the CW spinning resonator, the mechanical squeezing cannot be generated due to off-resonance. [The S for CCW driving is too small; we do not show it in Fig. 3(b).] It can be seen that by spinning the resonator, the absent squeezing can be significantly revived for $J/\kappa = 1$. Moreover, the maximum value of S can be further enhanced to that in an ideal resonator without backscattering by increasing the angular velocity, as shown in the inset of Fig. 3(b). That is, the presented scheme with large rotational angular velocity is immune to backscattering losses.

In addition, the squeezing of the mechanical oscillator will be inevitably influenced by mechanical thermal noise. We plot the degree of squeezing S (dB) versus the environmental temperature T and the scaled detuning Δ_c/ω_m in Fig. 4. The left and right sides in Fig. 4 correspond to the mechanical squeezing for the CW spinning resonator driven from the CCW and

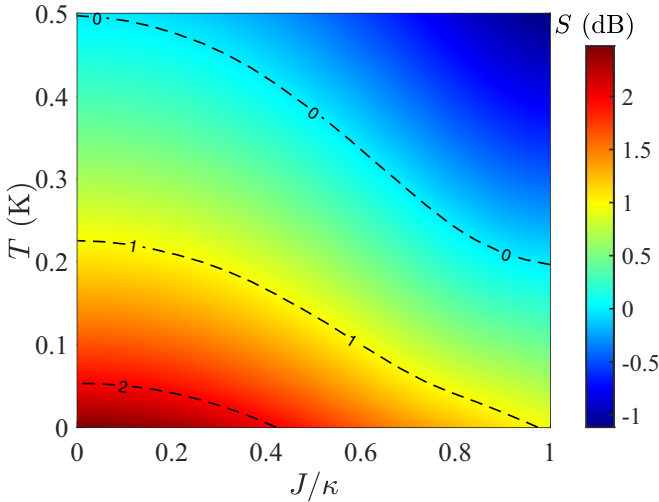


FIG. 5. The degree of squeezing S (dB) versus the environmental temperature T and the backscattering strength J when the spinning resonator is driven from the CW direction. Other parameters are the same as those in Fig. 3(b), except for $\Omega_0 = 8$ kHz.

CW directions, respectively, and the blank area indicates no mechanical squeezing occurs. Clearly, the nonreciprocity is not affected by the temperature, and the mechanical squeezing is present for a wide range of temperatures, even up to 450 mK. By taking into account both the backscattering losses and thermal noises, we numerically evaluate the robustness of the scheme in Fig. 5. Obviously, the degree of squeezing S (dB) will decrease with the increase of temperature T and backscattering J , but the mechanical squeezing can be generated within a large parameter region of T and J for a lower angular velocity of $\Omega_0 = 8$ kHz. According to the inset of Fig. 3(b), one can see the parameter region where the mechanical squeezing exists can be further expanded by increasing the angular velocity.

V. CONCLUSIONS

In conclusion, we have studied the nonreciprocal mechanical squeezing in a spinning COM system driven by a periodically modulated laser. Due to the optical Sagnac effect induced by spinning, the mechanical squeezing can be created by driving the resonator from one side, but no mechanical squeezing occurs by utilizing the same pump field to drive the resonator from the other side. We showed that the backscattering losses will have a serious impact on the mechanical squeezing for the spinning resonator with low angular velocities, but this impact can be completely eliminated by increasing the angular velocity of the resonator. We also evaluated the effect of the environmental temperature on nonreciprocal mechanical squeezing and found that the presented scheme has strong robustness to the mechanical thermal noise. The numerical results were obtained based on the feasible parameters of the current experiment. Note that the degree of the presented nonreciprocal mechanical squeezing can also break the 3-dB limit by coupling the spinning resonator to an ancilla cavity mode [46]. Therefore, this work may find potential applications in the study of quantum nonreciprocity,

macroscopic quantum phenomena, and direction-dependent quantum precision measurement.

ACKNOWLEDGMENTS

This work is supported by the National Natural Science Foundation of China under Grants No. 12274274, No. 11974223, No. U21A6006, and No. U21A20433 and by the National Key Research and Development Program of China under Grant No. 2021YFA1402002.

APPENDIX: THE ANALYSIS OF THE OPTIMAL MODULATION FREQUENCY AND THE EFFECTS OF DRIVING POWERS ON THE MECHANICAL SQUEEZING

Here we study the optimal fundamental modulation frequency and the effects of driving powers on the scheme. From the underlying physics of the scheme, one can see the pump modulation leads to the mechanical squeezing, while the spinning resonator and the driving direction induce the nonreciprocity. Therefore, in order to analyze the effects of driving powers P_0 and $P_{\pm 1}$ and the modulation frequency Ω , we here only consider the stationary resonator without backscattering, i.e., $\Delta_F = 0$ and $J = 0$, and the amplitude-modulated pump is used to drive the CCW cavity mode. Then the Hamiltonian in Eq. (2) can be written as ($\hbar = 1$)

$$\hat{H} = \omega_{\cup} \hat{a}_{\cup}^{\dagger} \hat{a}_{\cup} + \frac{\omega_m}{2} (\hat{p}^2 + \hat{q}^2) - G_0 \hat{a}_{\cup}^{\dagger} \hat{a}_{\cup} \hat{q} + i[E(t) \hat{a}_{\cup}^{\dagger} e^{-i\omega_l t} - E^*(t) \hat{a}_{\cup} e^{i\omega_l t}]. \quad (\text{A1})$$

In the rotating frame with respect to $\hat{H}_0 = \omega_l \hat{a}_{\cup}^{\dagger} \hat{a}_{\cup}$, the Hamiltonian of this COM system is

$$\hat{H} = \Delta_{\cup} \hat{a}_{\cup}^{\dagger} \hat{a}_{\cup} + \frac{\omega_m}{2} (\hat{p}^2 + \hat{q}^2) - G_0 \hat{a}_{\cup}^{\dagger} \hat{a}_{\cup} \hat{q} + i[E(t) \hat{a}_{\cup}^{\dagger} - E^*(t) \hat{a}_{\cup}], \quad (\text{A2})$$

where $\Delta_{\cup} = \omega_{\cup} - \omega_l$ is the detuning between the resonance frequency of the cavity field and the driving frequency. Under the condition of strong laser driving, the system operator can be written as the sum form: $\hat{a}_{\cup} = \alpha_{\cup} + \delta \hat{a}_{\cup}$, $\hat{q} = q_s + \delta \hat{q}$, $\hat{p} = p_s + \delta \hat{p}$. For convenience, we write $\delta \hat{O}$ as \hat{O} ($\hat{O} = \hat{a}_{\cup}$, \hat{q} , \hat{p}) and keep only quadratic terms; then the corresponding linearized system Hamiltonian can be obtained:

$$\hat{H} = \tilde{\Delta}_{\cup} \hat{a}_{\cup}^{\dagger} \hat{a}_{\cup} + \frac{\omega_m}{2} (\hat{p}^2 + \hat{q}^2) - G_0 (\alpha_{\cup}^* \hat{a}_{\cup} + \alpha_{\cup} \hat{a}_{\cup}^{\dagger}) \hat{q}, \quad (\text{A3})$$

where $\tilde{\Delta}_{\cup} = \Delta_{\cup} - G_0 q_s$ is the effective detuning.

Now we introduce the creation and annihilation operators of the mechanical fluctuations:

$$\hat{b} = (\hat{q} + i\hat{p})/\sqrt{2}, \quad \hat{b}^{\dagger} = (\hat{q} - i\hat{p})/\sqrt{2}. \quad (\text{A4})$$

Thus, the linearized system Hamiltonian can be rewritten as

$$\hat{H} = \tilde{\Delta}_{\cup} \hat{a}_{\cup}^{\dagger} \hat{a}_{\cup} + \omega_m \hat{b}^{\dagger} \hat{b} - \frac{1}{2} [g^*(t) \hat{a}_{\cup} + g(t) \hat{a}_{\cup}^{\dagger}] (\hat{b} + \hat{b}^{\dagger}), \quad (\text{A5})$$

where the effective COM coupling rate $g(t) = \sqrt{2} G_0 \alpha_{\cup}$. Since the modulation period of the pump is τ , according to Floquet's theorem, the asymptotic evolution of the system

will have the same period τ [39]. Without loss of generality, we can assume the asymptotic form for time-dependent mean values of the cavity modes as follows:

$$\alpha_{\cup} = \alpha_0 + \alpha_1 e^{-i\Omega t}, \quad (\text{A6})$$

and the effective COM coupling rate is

$$g(t) = \sqrt{2}G_0\alpha_{\cup} = \sqrt{2}G_0(\alpha_0 + \alpha_1 e^{-i\Omega t}) = g_0 + g_1 e^{-i\Omega t}. \quad (\text{A7})$$

In the rotating frame with respect to the free Hamiltonian $\tilde{\Delta}_{\cup}\hat{a}_{\cup}^{\dagger}\hat{a}_{\cup} + \omega_m\hat{b}^{\dagger}\hat{b}$, and choosing $\tilde{\Delta}_{\cup} = \omega_m$, the Hamiltonian in Eq. (A5) will become

$$\begin{aligned} \hat{H} = & -\frac{1}{2}[(g_0 e^{-2i\omega_m t} + g_1 e^{-i(2\omega_m - \Omega)t})\hat{a}_{\cup}\hat{b} \\ & + (g_0 + g_1 e^{i\Omega t})\hat{a}_{\cup}\hat{b}^{\dagger} + (g_0 + g_1 e^{-i\Omega t})\hat{a}_{\cup}^{\dagger}\hat{b} \\ & + (g_0 e^{2i\omega_m t} + g_1 e^{i(2\omega_m - \Omega)t})\hat{a}_{\cup}^{\dagger}\hat{b}^{\dagger}]. \end{aligned} \quad (\text{A8})$$

When $\omega_m, \Omega \gg g_0$, we can perform the rotating-wave approximation:

$$\begin{aligned} \hat{H} = & -\frac{1}{2}[g_1 e^{-i(2\omega_m - \Omega)t}\hat{a}_{\cup}\hat{b} + g_0\hat{a}_{\cup}\hat{b}^{\dagger} + g_0\hat{a}_{\cup}^{\dagger}\hat{b} \\ & + g_1 e^{i(2\omega_m - \Omega)t}\hat{a}_{\cup}^{\dagger}\hat{b}^{\dagger}] \\ = & -\frac{1}{2}\{g_1[\cos(2\omega_m - \Omega)t](\hat{a}_{\cup}\hat{b} + \hat{a}_{\cup}^{\dagger}\hat{b}^{\dagger}) \\ & + g_0(\hat{a}_{\cup}\hat{b}^{\dagger} + \hat{a}_{\cup}^{\dagger}\hat{b}) \\ & - ig_1[\sin(2\omega_m - \Omega)t](\hat{a}_{\cup}\hat{b} - \hat{a}_{\cup}^{\dagger}\hat{b}^{\dagger})\}. \end{aligned} \quad (\text{A9})$$

By introducing Bogoliubov-mode annihilation operators of the mechanical mode

$$\hat{\beta} = \hat{b} \cosh r + \hat{b}^{\dagger} \sinh r, \quad (\text{A10})$$

the Hamiltonian can be written as

$$\begin{aligned} \hat{H} = & -\frac{1}{2} \left\{ \frac{ig_1^2 \sin[2(2\omega_m - \Omega)t]}{\sqrt{g_0^2 - g_1^2 \cos[(2\omega_m - \Omega)t]}} \right. \\ & \left. + \sqrt{g_0^2 - g_1^2 \cos^2[(2\omega_m - \Omega)t]} \right\} (\hat{a}_{\cup}\hat{\beta}^{\dagger} + \hat{a}_{\cup}^{\dagger}\hat{\beta}) \\ & - \frac{ig_0g_1 \sin[(2\omega_m - \Omega)t]}{\sqrt{g_0^2 - g_1^2 \cos[(2\omega_m - \Omega)t]}} (\hat{a}_{\cup}\hat{\beta} + \hat{a}_{\cup}^{\dagger}\hat{\beta}^{\dagger}), \end{aligned} \quad (\text{A11})$$

where the squeezing parameter r is defined as $\tanh r = g_1 \cos[(2\omega_m - \Omega)t]/g_0$. According to the Routh-Hurwitz criterion [61], it can be demonstrated that the stability of the system requires $g_1 \cos[(2\omega_m - \Omega)t] < g_0$. The first term in the Hamiltonian above is the beam-splitter interaction between the cavity mode and the Bogoliubov mode, and the second term is their two-mode squeezing interaction. Because the ground state of the Bogoliubov mode $\hat{\beta}$ is the squeezing vacuum state of the mechanical mode, the beam-splitter interaction can be used to cool the Bogoliubov mode and thus generate the mechanical squeezing. When the modulation frequency $\Omega = 2\omega_m$, the above Hamiltonian is written as

$$H = -\frac{1}{2}\sqrt{g_0^2 - g_1^2}(\hat{a}_{\cup}\hat{\beta}^{\dagger} + \hat{a}_{\cup}^{\dagger}\hat{\beta}). \quad (\text{A12})$$

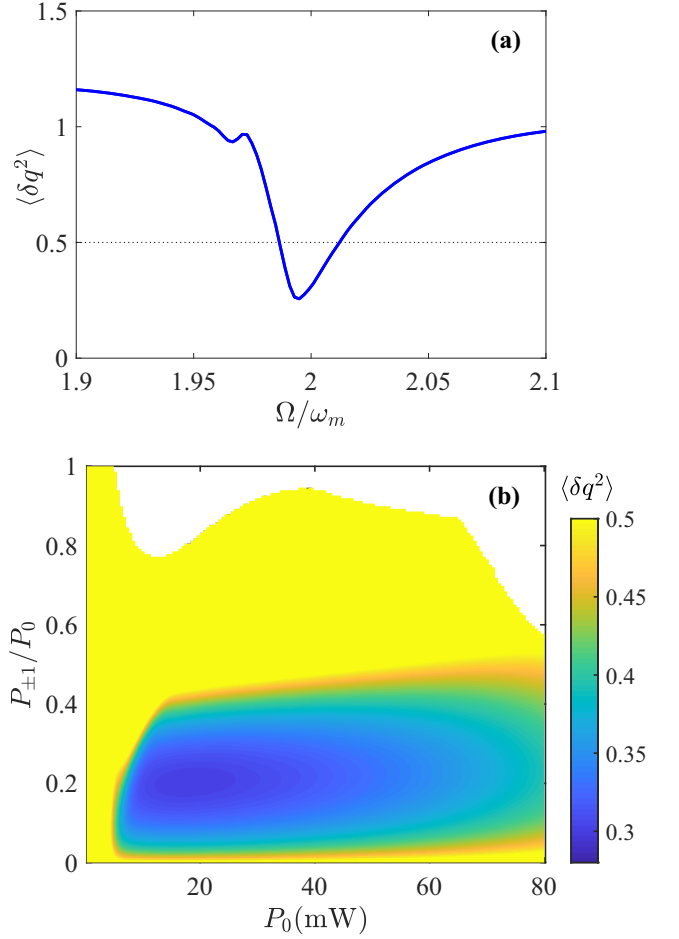


FIG. 6. (a) The position variance $\langle \delta q^2 \rangle$ of the mechanical mode versus the modulation frequency Ω . (b) $\langle \delta q^2 \rangle$ versus the carrier power P_0 and the sideband power $P_{\pm 1}$. The blank area indicates the unstable region of the system. The parameters are consistent with those in Fig. 2(b) for $\Delta_F = 0$.

Obviously, the two-mode squeezing interaction is eliminated; that is, the heating of the Bogoliubov mode is completely suppressed. Therefore, the condition $\Omega = 2\omega_m$ is optimal for the mechanical squeezing. We numerically plot the position variance $\langle \delta q^2 \rangle$ of the mechanical mode as a function of the modulation frequency Ω in Fig. 6(a), which shows the position variance is minimum at $\Omega = 2\omega_m$, consistent with the above theoretical analysis.

We numerically calculate the position variance $\langle \delta q^2 \rangle$ of the mechanical mode and plot it versus the driving powers P_0 and $P_{\pm 1}$ in Fig. 6(b), which shows there are also optimal values of P_0 and $P_{\pm 1}$ for the mechanical squeezing, though the amplitude-modulated pump plays an important role in the scheme. That can be explained as follows. From the derivation above, the condition $g_1 \cos[(2\omega_m - \Omega)t] < g_0 \ll \omega_m$ is required to obtain the effective Hamiltonian (A12), while g_0 and g_1 depend on the carrier power P_0 and the modulation power $P_{\pm 1}$, respectively. When the carrier power P_0 is too high, the condition $g_0 \ll \omega_m$ will not be satisfied, and thus the rotating-wave approximation for Eq. (A8) will be invalid and the counter-rotating wave terms will reduce the squeezing. When the modulation power $P_{\pm 1}$ is too high, on one hand, the

condition $g_1 \cos[(2\omega_m - \Omega)t] < g_0$ will not be satisfied, leading to the system's instability; on the other hand, the strength of beam-splitter interaction $\sqrt{g_0^2 - g_1^2}$ in Eq. (A12) will be

decreased, so the squeezing will also be reduced. Therefore, the numerical results agree well with the theoretical derivation above.

-
- [1] A. A. Maznev, A. G. Every, and O. B. Wright, Reciprocity in reflection and transmission: What is a ‘phonon diode’? *Wave Motion* **50**, 776 (2013).
- [2] B. I. Popa and S. A. Cummer, Non-reciprocal and highly nonlinear active acoustic metamaterials, *Nat. Commun.* **5**, 3398 (2014).
- [3] D. L. Sounas and A. Alù, Non-reciprocal photonics based on time modulation, *Nat. Photonics* **11**, 774 (2017).
- [4] D. Torrent, O. Poncelet, and J. C. Batsale, Nonreciprocal Thermal Material by Spatiotemporal Modulation, *Phys. Rev. Lett.* **120**, 125501 (2018).
- [5] Y. Shoji and T. Mizumoto, Magneto-optical non-reciprocal devices in silicon photonics, *Sci. Technol. Adv. Mater.* **15**, 014602 (2014).
- [6] Q.-T. Cao, H. Wang, C.-H. Dong, H. Jing, R.-S. Liu, X. Chen, and Y.-F. Xiao, Experimental Demonstration of Spontaneous Chirality in a Nonlinear Microresonator, *Phys. Rev. Lett.* **118**, 033901 (2017).
- [7] Q.-T. Cao, R. Liu, H. Wang, Y.-K. Lu, C.-W. Qiu, S. Rotter, and Y.-F. Xiao, Reconfigurable symmetry-broken laser in a symmetric microcavity, *Nat. Commun.* **11**, 1136 (2020).
- [8] K. Xia, F. Nori, and M. Xiao, Cavity-Free Optical Isolators and Circulators Using a Chiral Cross-Kerr Nonlinearity, *Phys. Rev. Lett.* **121**, 203602 (2018).
- [9] S. Manipatruni, J. T. Robinson, and M. Lipson, Optical Non-reciprocity in Optomechanical Structures, *Phys. Rev. Lett.* **102**, 213903 (2009).
- [10] M. Hafezi and P. Rabl, Optomechanically induced non-reciprocity in microring resonators, *Opt. Express* **20**, 7672 (2012).
- [11] Z. Shen, Y.-L. Zhang, Y. Chen, C.-L. Zou, Y.-F. Xiao, X.-B. Zou, and C.-H. Dong, Experimental realization of optomechanically induced non-reciprocity, *Nat. Photonics* **10**, 657 (2016).
- [12] N. R. Bernier, L. D. Toth, A. Koottandavida, M. A. Ioannou, D. Malz, A. Nunnenkamp, and T. J. Kippenberg, Nonreciprocal reconfigurable microwave optomechanical circuit, *Nat. Commun.* **8**, 604 (2017).
- [13] L. Mercier de Lépinay, E. Damskäg, C. F. Ockeloen-Korppi, and M. A. Sillanpää, Realization of Directional Amplification in a Microwave Optomechanical Device, *Phys. Rev. Appl.* **11**, 034027 (2019).
- [14] C.-H. Dong, Z. Shen, C.-L. Zou, Y.-L. Zhang, W. Fu, and G.-C. Guo, Brillouin-scattering-induced transparency and non-reciprocal light storage, *Nat. Commun.* **6**, 6193 (2015).
- [15] J. Kim, M.-C. Kuzuk, K. Han, H. Wang, and G. Bahl, Non-reciprocal Brillouin scattering induced transparency, *Nat. Phys.* **11**, 275 (2015).
- [16] M. Lawrence and J. A. Dionne, Nanoscale nonreciprocity via photon-spin-polarized stimulated Raman scattering, *Nat. Commun.* **10**, 3297 (2019).
- [17] P. Yang, X. Xia, H. He, S. Li, X. Han, P. Zhang, G. Li, P. Zhang, J. Xu, Y. Yang, and T. Zhang, Realization of Nonlinear Optical Nonreciprocity on a Few-Photon Level Based on Atoms Strongly Coupled to an Asymmetric Cavity, *Phys. Rev. Lett.* **123**, 233604 (2019).
- [18] Y. Shen, M. Bradford, and J.-T. Shen, Single-Photon Diode by Exploiting the Photon Polarization in a Waveguide, *Phys. Rev. Lett.* **107**, 173902 (2011).
- [19] S. Zhang, Y. Hu, G. Lin, Y. Niu, K. Xia, J. Gong, and S. Gong, Thermal-motion-induced non-reciprocal quantum optical system, *Nat. Photonics* **12**, 744 (2018).
- [20] M.-X. Dong, K.-Y. Xia, W.-H. Zhang, Y.-C. Yu, Y.-H. Ye, E.-Z. Li, and F. Nori, All-optical reversible single-photon isolation at room temperature, *Sci. Adv.* **7**, eabe8924 (2021).
- [21] M. Scheucher, A. Hilico, E. Will, J. Volz, and A. Rauschenbeutel, Quantum optical circulator controlled by a single chirally coupled atom, *Science* **354**, 1577 (2016).
- [22] R. Huang, A. Miranowicz, J.-Q. Liao, F. Nori, and H. Jing, Nonreciprocal Photon Blockade, *Phys. Rev. Lett.* **121**, 153601 (2018).
- [23] P. Yang, M. Li, X. Han, H. He, G. Li, C.-L. Zou, P. Zhang, Y. Qian, and T. Zhang, Non-reciprocal cavity polariton with atoms strongly coupled to optical cavity, *Laser Photonics Rev.* **17**, 2200574 (2023).
- [24] J.-S. Tang, W. Nie, L. Tang, M. Chen, X. Su, Y. Lu, F. Nori, and K. Xia, Nonreciprocal Single-Photon Band Structure, *Phys. Rev. Lett.* **128**, 203602 (2022).
- [25] S.-Y. Ren, W. Yan, L.-T. Feng, Y. Chen, Y.-K. Wu, X.-Z. Qi, X.-J. Liu, Y.-J. Cheng, B.-Y. Xu, L.-J. Deng, G.-C. Guo, L. Bi, and X.-F. Ren, Single-photon nonreciprocity with an integrated magneto-optical isolator, *Laser Photonics Rev.* **16**, 2100595 (2022).
- [26] H. Lü, Y. Jiang, Y.-Z. Wang, and H. Jing, Optomechanically induced transparency in a spinning resonator, *Photonics Res.* **5**, 367 (2017).
- [27] S. Maayani, R. Dahan, Y. Kligerman, E. Moses, A. U. Hassan, H. Jing, and T. Carmon, Flying couplers above spinning resonators generate irreversible refraction, *Nature (London)* **558**, 569 (2018).
- [28] Y. Jiao, C.-H. Bai, D.-Y. Wang, S. Zhang, and H.-F. Wang, Optical nonreciprocal response and conversion in a Tavis-Cummings coupling optomechanical system, *Quantum Eng.* **2**, e39 (2020).
- [29] Y.-F. Jiao, S.-D. Zhang, Y.-L. Zhang, A. Miranowicz, L.-M. Kuang, and H. Jing, Nonreciprocal Optomechanical Entanglement against Backscattering Losses, *Phys. Rev. Lett.* **125**, 143605 (2020).
- [30] Y.-F. Jiao, J.-X. Liu, Y. Li, R. Yang, L.-M. Kuang, and H. Jing, Nonreciprocal Enhancement of Remote Entanglement between Nonidentical Mechanical Oscillators, *Phys. Rev. Appl.* **18**, 064008 (2022).
- [31] Y. Jiang, S. Maayani, T. Carmon, F. Nori, and H. Jing, Nonreciprocal Phonon Laser, *Phys. Rev. Appl.* **10**, 064037 (2018).
- [32] Y. Xu, J.-Y. Liu, W. Liu, and Y.-F. Xiao, Nonreciprocal phonon laser in a spinning microwave magnomechanical system, *Phys. Rev. A* **103**, 053501 (2021)

- [33] B. Li, R. Huang, X. Xu, A. Miranowicz, and H. Jing, Nonreciprocal unconventional photon blockade in a spinning optomechanical system, *Photonics Res.* **7**, 630 (2019).
- [34] Y.-M. Liu, J. Cheng, H.-F. Wang, and X. Yi, Nonreciprocal photon blockade in a spinning optomechanical system with nonreciprocal coupling, *Opt. Express* **31**, 12847 (2023).
- [35] S. S. Chen, S. S. Meng, H. Deng, and G. J. Yang, Nonreciprocal mechanical squeezing in a spinning optomechanical system, *Ann. Phys.* **533**, 2000343 (2021).
- [36] M. J. Woolley, A. C. Doherty, G. J. Milburn, and K. C. Schwab, Nanomechanical squeezing with detection via a microwave cavity, *Phys. Rev. A* **78**, 062303 (2008).
- [37] G. S. Agarwal and S. Huang, Strong mechanical squeezing and its detection, *Phys. Rev. A* **93**, 043844 (2016).
- [38] A. Kronwald, F. Marquardt, and A. A. Clerk, Arbitrarily large steady-state bosonic squeezing via dissipation, *Phys. Rev. A* **88**, 063833 (2013).
- [39] A. Mari and J. Eisert, Gently Modulating Optomechanical Systems, *Phys. Rev. Lett.* **103**, 213603 (2009).
- [40] A. Mari and J. Eisert, Opto-and electro-mechanical entanglement improved by modulation, *New J. Phys.* **14**, 075014 (2012).
- [41] W.-J. Gu and G.-X. Li, Squeezing of the mirror motion via periodic modulations in a dissipative optomechanical system, *Opt. Express* **21**, 20423 (2013).
- [42] R.-X. Chen, L.-T. Shen, Z.-B. Yang, H.-Z. Wu, and S.-B. Zheng, Enhancement of entanglement in distant mechanical vibrations via modulation in a coupled optomechanical system, *Phys. Rev. A* **89**, 023843 (2014).
- [43] M. Abdi and M. J. Hartmann, Entangling the motion of two optically trapped objects via time-modulated driving fields, *New J. Phys.* **17**, 013056 (2015).
- [44] C.-H. Bai, D.-Y. Wang, S. Zhang, S. Liu, and H.-F. Wang, Strong mechanical squeezing in a standard optomechanical system by pump modulation, *Phys. Rev. A* **101**, 053836 (2020).
- [45] C.-H. Bai, D.-Y. Wang, S. Zhang, S. Liu, and H.-F. Wang, Modulation-based atom-mirror entanglement and mechanical squeezing in an unresolved-sideband optomechanical system, *Ann. Phys.* **531**, 1800271 (2019).
- [46] W.-J. Zhang, Y.-C. Zhang, Q. Guo, A.-P. Liu, G. Li, and T.-C. Zhang, Strong mechanical squeezing and optomechanical entanglement in a dissipative double-cavity system via pump modulation, *Phys. Rev. A* **104**, 053506 (2021).
- [47] M. Schmidt, M. Ludwig, and F. Marquardt, Optomechanical circuits for nanomechanical continuous variable quantum state processing, *New J. Phys.* **14**, 125005 (2012).
- [48] X.-Y. Lü, J.-Q. Liao, L. Tian, and F. Nori, Steady-state mechanical squeezing in an optomechanical system via Duffing nonlinearity, *Phys. Rev. A* **91**, 013834 (2015).
- [49] D.-Y. Wang, C.-H. Bai, H.-F. Wang, A.-D. Zhu, and S. Zhang, Steady-state mechanical squeezing in a double-cavity optomechanical system, *Sci. Rep.* **6**, 38559 (2016).
- [50] M. Wang, X.-Y. Lü, Y.-D. Wang, J.-Q. You, and Y. Wu, Macroscopic quantum entanglement in modulated optomechanics, *Phys. Rev. A* **94**, 053807 (2016).
- [51] B. Rogers, M. Paternostro, G. M. Palma, and G. De Chiara, Entanglement control in hybrid optomechanical systems, *Phys. Rev. A* **86**, 042323 (2012).
- [52] P. Doria, T. Calarco, and S. Montangero, Optimal Control Technique for Many-Body Quantum Dynamics, *Phys. Rev. Lett.* **106**, 190501 (2011).
- [53] G. B. Malykin, The Sagnac effect: Correct and incorrect explanations, *Phys.-Usp.* **43**, 1229 (2000).
- [54] M. Aspelmeyer, T. J. Kippenberg, and F. Marquardt, Cavity optomechanics, *Rev. Mod. Phys.* **86**, 1391 (2014).
- [55] T. J. Kippenberg, S. M. Spillane, and K. J. Vahala, Modal coupling in traveling-wave resonators, *Opt. Lett.* **27**, 1669 (2002).
- [56] S. Kim, J. M. Taylor, and G. Bahl, Dynamic suppression of Rayleigh backscattering in dielectric resonators, *Optica* **6**, 1016 (2019).
- [57] C. W. Gardiner and P. Zoller, *Quantum Noise*, 3rd ed. (Springer, New York, 2004).
- [58] V. Giovannetti and D. Vitali, Phase-noise measurement in a cavity with a movable mirror undergoing quantum Brownian motion, *Phys. Rev. A* **63**, 023812 (2001).
- [59] A. A. Clerk, M. H. Devoret, S. M. Girvin, F. Marquardt, and R. J. Schoelkopf, Introduction to quantum noise, measurement, and amplification, *Rev. Mod. Phys.* **82**, 1155 (2010).
- [60] C. Weedbrook, S. Pirandola, R. García-Patrón, N. J. Cerf, T. C. Ralph, J. H. Shapiro, and S. Lloyd, Gaussian quantum information, *Rev. Mod. Phys.* **84**, 621 (2012).
- [61] E. X. DeJesus and C. Kaufman, Routh-Hurwitz criterion in the examination of eigenvalues of a system of nonlinear ordinary differential equations, *Phys. Rev. A* **35**, 5288 (1987).
- [62] G. C. Righini, Y. Dumeige, P. Féron, M. Ferrari, G. Nunzi Conti, D. Ristic, and S. Soria, Whispering gallery mode microresonators: Fundamentals and applications, *Riv. Nuovo Cimento* **34**, 435 (2011).
- [63] A. Mazzei, S. Götzinger, L. D. S. Menezes, G. Zumofen, O. Benson, and V. Sandoghdar, Controlled Coupling of Counter-propagating Whispering-Gallery Modes by a Single Rayleigh Scatterer: A Classical Problem in a Quantum Optical Light, *Phys. Rev. Lett.* **99**, 173603 (2007).
- [64] Y. Chen, Z. Shen, X. Xiong, C.-H. Dong, C.-L. Zou, and G.-C. Guo, Mechanical bound state in the continuum for optomechanical microresonators, *New J. Phys.* **18**, 063031 (2016).